Non-collinear magnetic order in nanostructures investigated by spin-polarized scanning tunneling microscopy*

Oswald Pietzsch[‡] and Roland Wiesendanger

Institute of Applied Physics, University Hamburg, Jungiusstraße 9-11, 20355 Hamburg, Germany

Abstract: The successful conjunction of the ultimate spatial resolution capability of the scanning tunneling microscope (STM) with the sensitivity to the spin of the tunneling electrons has opened the door to investigations of magnetism at the nanoscale where the fundamental interactions responsible for magnetic order can be studied. Spin-polarized (SP) STM allows insight into a fascinating world with surprisingly rich magnetic phenomena. Ferromagnetic structures with magnetic domains are found at nanometer length scales, or 2D antiferromagnetically ordered monolayers (MLs) where the magnetization is reversed from one atom to the next. Such collinearly ordered states may be modified by the Dzyaloshinsky–Moriya (DM) interaction which can induce a small canting angle between neighboring atomic moments, thus giving rise to novel non-collinear spin spiral ground states. DM interaction is a result of electron scattering in a crystal environment with broken inversion symmetry. Spin spirals were observed in a variety of systems, like ultrathin Fe films, or MLs of Mn atoms on the (110) and (001) faces of a W crystal. Using a magnetically sensitive probe tip, individual Co atoms were assembled to form chains on top of a spin spiral. The magnetization orientation of each individual atom can be manipulated by repositioning it along the spin spiral.

Keywords: magnetic properties; scanning tunneling microscopy (STM); nanostructures; thin films; transition metals.

INTRODUCTION

Spin-polarized scanning tunneling microscopy

Spin-polarized tunneling was first observed by Jullière using planar tunnel junctions [1]. He investigated the tunneling conductance between two ferromagnetic films separated by a thin insulating layer. For a parallel alignment of the magnetic electrodes a higher conductance was observed than for the antiparallel case. Slonczewski developed an expression for the tunneling current [2], which can be applied also in spin-polarized scanning tunneling microscopy (SP-STM)

$$I_{SP}(V_0, \eta_\parallel) \propto I_0 \cdot [1 + P_{tip} \cdot P_{sample} \cdot \cos \theta(\eta_\parallel)] \tag{1}$$

The tunneling current I_{SP} at a bias voltage V_0 consists of one part that is not spin-polarized, and a second part that depends on the spin polarizations P of the two electrodes, i.e., here tip and sample, times

---

the cosine of the angle θ between the magnetization vectors of tip and sample at the position $r_\parallel$ of the tip. This latter cosine dependence has been confirmed experimentally for planar tunneling junctions by Miyazaki and Tezuka [3] and is essential for the contrast mechanism in SP-STM. The achievable contrasts are maximized for parallel vs. antiparallel configurations while contrast vanishes for an orthogonal arrangement.

While eq. 1 is particularly useful when imaging magnetic structures at the length scale of the atomic lattice, a similar expression can be given for the differential conductance $dI/dV(V)$, which is the quantity measured most conveniently for domain imaging

$$dI/dV_{SP}(V,r_\parallel) \propto G(V) \cdot [1 + P_{tip} \cdot P_{sample} \cdot \cos\theta(r_\parallel)] \tag{2}$$

with $G(V)$ the differential conductance at an energy $E_F + eV$, which is proportional to the local density of states at this energy. Both modes of SP-STM operation will be used in the following.

Spin sensitivity of the tunneling tips is achieved by coating electrochemically etched tungsten tips with thin films of magnetic material. Fe coating results in a tip magnetization oriented perpendicular to the tip axis, thus giving in-plane sensitivity, whereas coating with Gd or Cr gives rise to a magnetization along the tip axis, i.e., sensitivity to the sample's out-of-plane magnetization component.

Dzyaloshinsky–Moriya (DM) interaction

In collinear metallic thin films exhibiting ferromagnetic or antiferromagnetic order, in many cases it is sufficient to consider local energy contributions arising from isotropic Heisenberg exchange and anisotropy energy

$$E_H = \sum_{i,j} J_{ij} S_i \cdot S_j, \qquad E_{Ani} = \sum_i K_i \sin^2\varphi \tag{3}$$

The leading term is the Heisenberg exchange interaction between magnetic spin moments S located on atomic sites i and j. Depending on the sign of the coupling constant J_{ij} this term favors ferromagnetic or antiferromagnetic coupling of neighboring spins, i.e., a collinear structure. The anisotropy term arises from relativistic spin-orbit coupling (SOC) and relates the direction of the spin moment at site i to a certain crystallographic axis, with a coupling constant K_i this term is responsible for the occurrence of easy and hard magnetic directions, with φ the angle between the local magnetization and the easy direction. For ferromagnetic systems, magnetostatic interactions also have to be included, which also contribute to the effective anisotropy via shape anisotropy.

None of these symmetric contributions to the total energy lend themselves to generating a magnetic ground state that is a spiral with a unique sense of spin rotation. Such a term was introduced by Dzyaloshinsky [4] and Moriya [5], hence DM interaction

$$E_{DM} = \sum_{i,j} D_{ij} \left(S_i \times S_j \right) \tag{4}$$

In contrast to eq. 3, this term describes an antisymmetric interaction, resulting from SOC, which connects the lattice with the spin symmetry. If the lattice possesses inversion symmetry, the DM term immediately vanishes. However, at a surface or an interface inversion symmetry is always broken and DM may thus be relevant. In this case, the DM term directly competes with the Heisenberg term, indicating that energy may be saved by deviating from a collinear spin alignment by introducing an angle ϕ between spins i and j. Further, energy will be lowered only if the spin rotation is in the proper direction (depending on the sign of D), while rotation in the opposite direction increases the total energy. Thus, DM provides a mechanism allowing the understanding of the occurrence of spin spirals with a unique sense of spin rotation.

In the following, two quite different examples of spin spirals will be discussed. First, a system of double layer (DL) stripes of Fe on a stepped W(110) surface is presented, with ferromagnetic Heisenberg coupling and uniaxial perpendicular anisotropy. Next, a monolayer (ML) of Mn on the W(110) surface is discussed. Here the Heisenberg coupling is antiferromagnetic and the easy axis is in-plane. Finally, the latter Mn system is used as a template to control the magnetic properties of single adsorbed Co atoms.

INHOMOGENEOUS RIGHT-ROTATING SPIN SPIRAL IN Fe/W(110)

The system of 1.5 pseudomorphic layers Fe epitaxially grown on a bcc single-crystal W(110) surface has become an icon in the field of SP-STM. Prior to SP-STM application to Fe/W(110), spatially averaging methods, in particular magneto-optical Kerr effect (MOKE) measurements, had been used to successfully clarify some basic magnetic properties. It was recognized that areas covered with an ML of Fe atoms are magnetized in-plane with an easy axis along [1$\bar{1}$0] [6], whereas DL areas exhibit a magnetization perpendicular to the surface plane, leading to a "nanoscale switching of magnetic anisotropy" [7]. In stripe geometry, adjacent DL stripes were found to couple antiparallel due to dipolar interaction [6]. However, further details of the magnetic structure remained inaccessible, given the limited spatial resolution of the available methods.

This limitation was eventually overcome by the use of SP-STM. Starting in 2000, a series of studies were published investigating in great detail the magnetic properties and the underlying spin-resolved electronic structure of 1.5 ML Fe on W(110), and, by the same token, exploring the range of applicability of SP-STM. In DL areas, perpendicular domain structures were observed in stripe [8] and island morphologies [9], with typical domain wall widths of about 6 nm. A complete hysteresis loop was observed, imaging domain wall motion, domain creation, and annihilation at the nanometer scale [10]. A residual domain with strongly enhanced stability against remagnetization was found; using STM tips with a sensitivity to the in-plane magnetization component [11,12], these residual domains could be identified to consist of two 180° walls with the spins pointing in opposite directions in the centers of the partial walls, thus forming a 360° wall compressed by the external field. The stability and response to perpendicular fields was investigated in detail [12,13]. While in narrow DL stripes several hundred nm long domains in adjacent stripes were coupled antiferromagnetically by dipolar interactions, stripes exhibiting a width larger than about 14 nm show regular domain lengths of only 16–18 nm. Along [001], a periodicity of magnetic order of about 44 nm was observed.

Very early, this latter structure was recognized to be a spin spiral propagating along the [001] crystallographic direction [12]. Even more peculiar, only one unique sense of spin rotation was observed in these spirals, without exceptions. Three important questions remained open: (i) Are the domain walls of the Bloch or of the Néel type—or, to speak in terms of a spiral, is it a helix or a cycloid? (ii) What is the sense of spin rotation—left or right? (iii) Most important: what is the mechanism driving the spiral formation? These questions were recently addressed theoretically [14] and experimentally [15]. Here we focus on the experimental results.

In SP-STM experiments the desired sensitivity to the perpendicular or the in-plane component of the sample magnetization can be chosen by a proper selection of the magnetic coating material for the tunneling tip. Further, by application of a perpendicular external magnetic field another degree of freedom was available, allowing, e.g., the tip's sensitivity to change from in-plane to out-of-plane. So far, however, it was not possible to control the azimuthal orientation of the tip magnetization. But this is a prerequisite to determine the character of the spin spiral.

Only recently a new versatile SP-STM set-up became available. As a special feature, the system is equipped with an external vector field magnet allowing magnetic fields to be applied in any desired direction [16]. This set-up can be used to control the in-plane orientation of the tunneling tip's magnetization.

This feature is demonstrated in Fig. 1. In panels (a) and (c), the field and thus the tip magnetization is directed in-plane parallel to the [001] surface crystallographic axis (see arrows 'B') while in (b) and (d) the orientation is parallel to the [1$\bar{1}$0] axis. In (a) and (c), strong contrasts reveal the locations of the domain walls where the spins locally lie in the sample plane. Note the contrast reversal from (a) to (c) due to the reversal of the tip magnetization. These contrasts vanish when the field is applied along [1$\bar{1}$0], see panels (b) and (d), indicating that now tip and sample magnetizations are in an orthogonal configuration. This allows the conclusion that the domain walls are of the Néel type and not of the Bloch type as indicated in the inset of panel (d). In terms of a spin spiral, we now already know that it is a cycloid rather than a helix.

However, the sense of rotation has yet to be determined. For this we need to know the spin orientation in the domains. By applying the field perpendicular to the sample plane in upward direction it is observed that domains grow or shrink in size, depending on their spin orientation being parallel or antiparallel to the applied field, as can be seen in panel (e) of Fig. 1. As sketched in the inset of (e), the cycloid can now be identified as right-rotating, in qualitative agreement to ref. [14].

The angle of spin rotation along the propagation direction is not constant but varies as a function of position, $\phi = \phi(x)$. The canting angle between adjacent spins is smaller in the domains and larger in the walls. Hence, the Fe DL system is an inhomogeneous right-rotating cycloidal spin spiral.
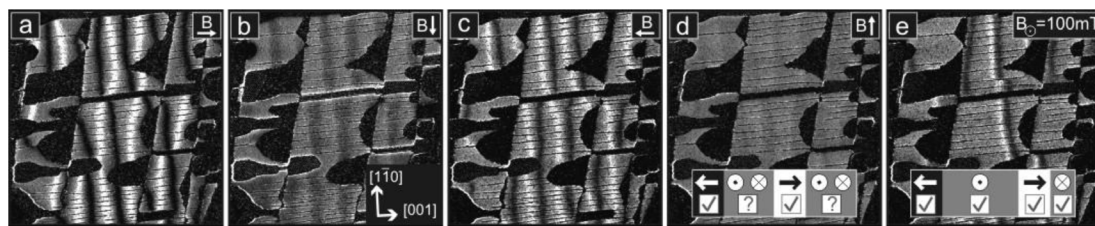

Fig. 1 1.6 ML Fe on W(110). Gray areas: DL thickness with perpendicular magnetization and domain walls (black and white lines visible in panels(a), (c), and (e)). External magnetic field applied in the surface plane ((a)–(d)) as indicated by arrows 'B'. In (e) the field is applied perpendicularly. Inset in (d): measurements (a)–(d) confirm the spins to point along the in-plane [001] rather than the [1$\bar{1}$0] axis. Inset in (e): The perpendicular field also allows the up and down domains to be distinguished, completing the information necessary to determine the right-handed sense of spin rotation.

SPIRALING A 2D ANTIFERROMAGNETIC STRUCTURE: Mn MONOLAYER ON W(110)

Based on density functional theory (DFT) investigations, the existence of 2D antiferromagnetically ordered overlayers of V, Cr, and Mn with an ultimate thickness of just one atomic layer on a Pd(001) surface was predicted in 1988 [17]. In these MLs it was expected to find the $p(1 \times 1)$ *chemical* unit cell, but also a $c(2 \times 2)$ *magnetic* unit cell, that is, the magnetic moments are reversed from one atom to the next. Experimentally, the challenge to observe such a structure was to find a method capable of atomic resolution with simultaneous spin sensitivity. This was eventually achieved by SP-STM in 2000 [18]. Figure. 2 shows a single Mn layer grown on a W(110) surface. The left image was taken with a non-magnetic W tip, resolving the atomic lattice of the pseudomorphic Mn ML. The right image was recorded with a tip coated with Fe being sensitive to the in-plane magnetization component of the sample. This time a pattern of bright and dark vertical rows is observed. This is due to the Mn moments being oriented parallel to the tip magnetic moment in one row (bright) and antiparallel in the next row (dark), in accord with a $c(2 \times 2)$ superstructure as sketched in the top left corner. This finding was in perfect agreement with simulated STM images based on spin-resolved DFT calculations. For the first time, spin contrast was achieved at the atomic length scale.
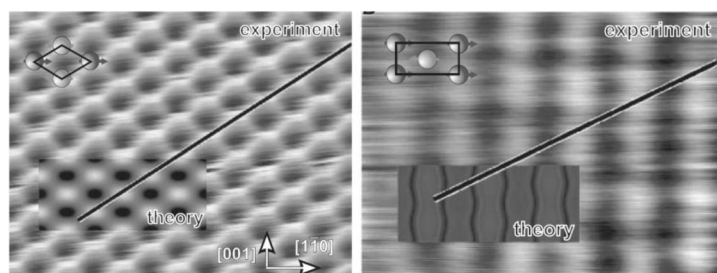
Fig. 2 A single Mn layer on W(110). Left: measurement with nonmagnetic W tip. The $p(1 \times 1)$ chemical lattice is resolved. Right: magnetic tip: a pattern of bright and dark lines reveals the antiferromagnetic $c(2 \times 2)$ magnetic superstructure.

The system Mn/W(110) was recently revisited with SP-STM in applied magnetic fields [19]. Next to the bright-and-dark line pattern with atomic-scale period described above, an additional modulation of the corrugation was observed, with a much larger period of about 6 nm between the nodes. As can be seen in Fig. 3, areas of high corrugation change periodically with areas of low corrugation. For the respective measurement again a Fe coated tip was used. In order to investigate the origin of the long wavelength modulation variable magnetic fields up to $B = 2$ T were applied perpendicular to the sample plane. The antiferromagnetic Mn film is not affected by the field because all magnetic moments are compensated. However, the moments of the ferromagnetic Fe tip, being in-plane at zero field, follow the increasing field from a horizontal into a vertical orientation. In the images this translates into a lateral shift of the long-wavelength feature. This observation can be explained by a cycloidal spin spiral in the Mn film if we take the change in sensitivity of the magnetic tip into account. While in zero field contrast is achieved at locations with sample moments lying in-plane, these contrasts vanish there, according to eq. 1, with the tip magnetization forced into the vertical direction. With this tip, however, contrasts appear at areas with sample moments pointing up and down.
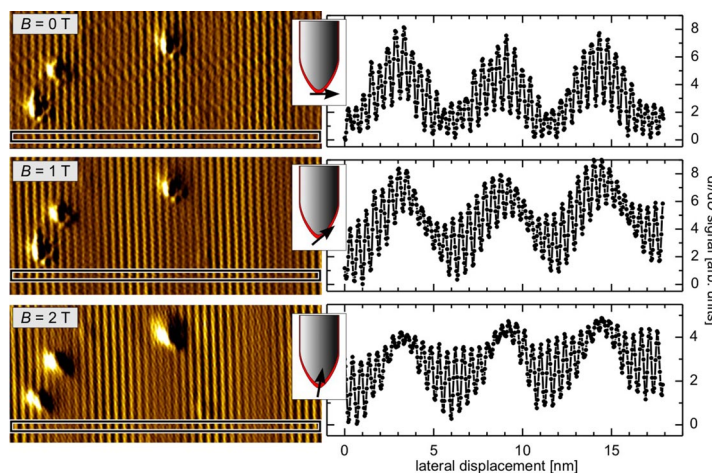

Fig. 3 SP-STM measurements of Mn/W(110) with a Fe-coated tip in variable external magnetic fields. The tip magnetization is rotated from horizontal to vertical. In the images, this appears as a lateral shift of the high-corrugation areas.

This finding was confirmed by DFT calculations [19]. While calculations neglecting SOC found the collinear antiferromagnetic solution to possess the lowest energy, inclusion of SOC—and thereby also DM interaction—resulted in a lower global energy minimum for a left-handed cycloidal spin spiral propagating along [1$\bar{1}$0] with a period of about 8 nm, in reasonable agreement to the experimental value of 12 nm (2 nodes to be considered because of the antiferromagnetic structure). The canting angle ϕ between adjacent moments can thus be determined to 173º.

ATOM MANIPULATION ON A SPIN SPIRAL AS TEMPLATE

Single magnetic adatoms have been studied by SP-STM on nonmagnetic metallic substrates [20] and also on magnetic surfaces [21]. Co atoms deposited on Pt(111) were found to rapidly switch their magnetic moments even at temperature as low as 300 mK, and only by application of strong magnetic fields was it possible to induce an imbalance in residence time between up and down states, allowing for the first time to measure magnetization curves of individual magnetic atoms. On a magnetic surface, on the other hand, the moment of a magnetic adatom will be stabilized up or down by exchange coupling to the substrate in either a ferromagnetic or an antiferromagnetic manner.

A new approach to stabilize the magnetization of single atoms has recently been demonstrated [22]. The spin spiral structure of Mn/W(110) can be used as a template, opening new possibilities to control and manipulate the orientation of the magnetic moments of individual atoms. Figure 4a shows individual Co monomers deposited at low temperatures ($T < 20$ K) onto the Mn film (a rare dimer is x-marked). Although chemically identical, they are imaged in a variety of shapes and heights, which can be systematically attributed to the relative alignment of their magnetizations to that of the magnetic tip. Panels (b) and (c) allow a comparison of Co atoms positioned on a bright (b) and the neighboring dark Mn row (c). Particularly striking is the clear difference in the observed symmetries: atom (b) shows rotational symmetry while it is two-fold for atom (c). This peculiar phenomenon has been scrutinized with spin-resolved DFT calculations [22], a method capable of addressing separately the majority and minority spin channels of the electronic band structure. According to these calculations, the atoms occupy bridge sites on their respective row. They couple ferromagnetically to their carrier row, so the magnetic moments of the atoms in Figs. 4(b), (c) are oriented (nearly) opposite. Therefore, tunneling proceeds preferentially into the majority, or the minority spin channel, respectively. The orbitals available for tunneling, however, exhibit quite different symmetries: while the majority spin channel is dom-
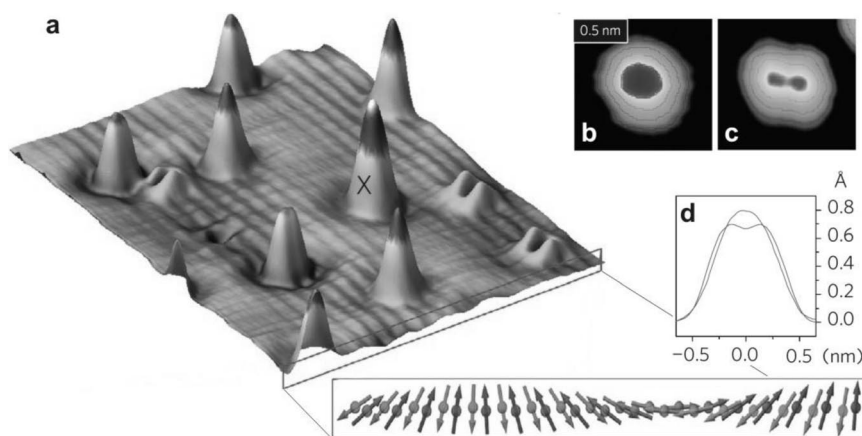

Fig. 4 (a) Single Co atoms on top of the Mn/W(110) spin spiral as imaged by a magnetic tip. Atoms positioned on a bright (b) and the nearest-neighbor dark Mn row (c). They differ significantly in height and shape, as can also be seen in the corresponding line sections (d).

inated by hybridized s, p_z, and $d_z{}^2$ orbitals—all of them being rotationally symmetric, the predominant minority orbital has d_{xz} character, that is, there are two lobes pointing into the vacuum region, directed away from the nucleus. This finding explains the observed differences in shape.

While the configurations shown in Figs. 4(b), (c) are the limiting cases of (nearly) opposite spin orientations, there are a variety of other possible orientations, depending on the position of a Co atom along the propagation direction of the Mn spin spiral. In order to study this effect in a systematic manner, a chain of Co atoms was assembled by using the tunneling tip to move individual Co atoms across the Mn surface into predefined equidistant positions. This type of atom manipulation is a well-established technique [23,24]. The challenge here was, however, to move the atoms without losing the spin sensitivity of the tip, which was successfully demonstrated for the first time in this experiment. The resulting chain is shown in Fig. 5. The Co atoms are 6 Mn rows apart. This corresponds to a spin rotation of about 42° from one atom to the next. By applying bipolar magnetic fields of 2.5 T as indicated by arrows, the orientation of the tip magnetic moment is controlled while the Mn film, possessing a zero net magnetic moment, remains unaffected, and so do the strongly coupled Co adatoms. Thus, the applied field reverses the magnetic tip, which acts as a spin filter, leading to characteristic changes in the appearances of the individual atoms.
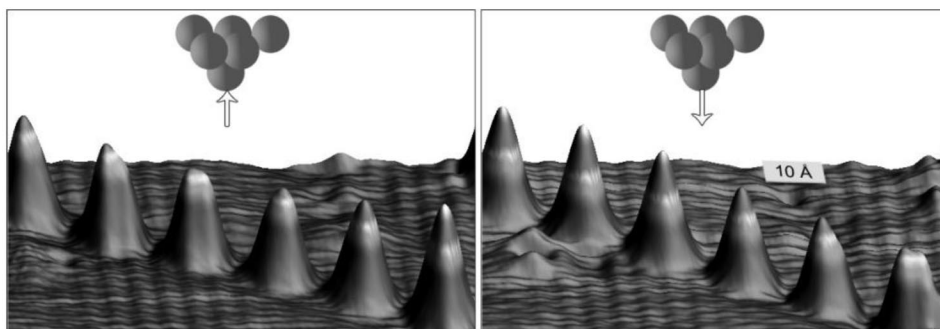

Fig. 5 Chain of Co atoms on the Mn spin spiral assembled by moving the atoms with the tunneling tip. Arrows indicate the direction of the magnetic field applied, $|B_z| = 2.5$ T. Fields are too weak to affect the antiferromagnetic structure with the strongly coupled Co atoms on top but fully align the ferromagnetic tip. Spacing between two atoms is 6 Mn rows, changing the magnetization angle by about 42°.

By moving a Co atom to the proper position on the Mn spin spiral, it is thus possible to orient its magnetic moment in virtually any desired direction within a plane given by the [1$\bar{1}$0] propagation direction and the surface normal. In summary, opportunities to control the single atom spin have reached a new level.

ACKNOWLEDGMENTS

REFERENCES

1. M. Julliere. *Phys. Lett. A* **54**, 225 (1975).
2. J. Slonczewski. *Phys. Rev. B* **39**, 6995 (1989).
3. T. Miyazaki, N. Tezuka. *J. Magn. Magn. Mater.* **139**, L231 (1995).
4. I. Dzyaloshinsky. *J. Phys. Chem. Solids* **4**, 241 (1958).
5. T. Moriya. *Phys. Rev. Lett.* **4**, 228 (1960).
6. J. Hauschild, U. Gradmann, H. J. Elmers. *Appl. Phys. Lett.* **72**, 3211 (1998).
7. N. Weber, K. Wagner, H. J. Elmers, J. Hauschild, U. Gradmann. *Phys. Rev. B* **55**, 14121 (1997).
8. O. Pietzsch, A. Kubetzka, M. Bode, R. Wiesendanger. *Phys. Rev. Lett.* **84**, 5212 (2000).
9. A. Kubetzka, O. Pietzsch, M. Bode, R. Wiesendanger. *Phys. Rev. B* **63**, 140407 (2001).
10. O. Pietzsch, A. Kubetzka, M. Bode, R. Wiesendanger. *Science* **292**, 2053 (2001).
11. M. Bode, O. Pietzsch, A. Kubetzka, S. Heinze, R. Wiesendanger. *Phys. Rev. Lett.* **86**, 2142 (2001).
12. A. Kubetzka, M. Bode, O. Pietzsch, R. Wiesendanger. *Phys. Rev. Lett.* **88**, 057201 (2002).
13. A. Kubetzka, O. Pietzsch, M. Bode, R. Wiesendanger. *Phys. Rev. B* **67**, 020401 (2003).
14. M. Heide, G. Bihlmayer, S. Blügel. *Phys. Rev. B* **78**, 140403 (2008).
15. S. Meckler, N. Mikuszeit, A. Preßler, E. Vedmedenko, O. Pietzsch, R. Wiesendanger. *Phys. Rev. Lett.* **103**, 157201 (2009).
16. S. Meckler, M. Gyamfi, O. Pietzsch, R. Wiesendanger. *Rev. Sci. Instrum.* **80**, 023708 (2009).
17. S. Blügel, M. Weinert, P. Dederichs. *Phys. Rev. Lett.* **60**, 1077 (1988).
18. S. Heinze, M. Bode, A. Kubetzka, O. Pietzsch, X. Nie, S. Blügel, R. Wiesendanger. *Science* **288**, 1805 (2000).
19. M. Bode, M. Heide, K. von Bergmann, P. Ferriani, S. Heinze, G. Bihlmayer, A. Kubetzka, O. Pietzsch, S. Blügel, R. Wiesendanger. *Nature* **447**, 190 (2007).
20. F. Meier, L. Zhou, J. Wiebe, R. Wiesendanger. *Science* **320**, 82 (2008).
21. Y. Yayon, V. W. Brar, L. Senapati, S. C. Erwin, M. F. Crommie. *Phys. Rev. Lett.* **99**, 067202 (2007).
22. D. Serrate, P. Ferriani, Y. Yoshida, S.-W. Hla, M. Menzel, K. von Bergmann, S. Heinze, A. Kubetzka, R. Wiesendanger. *Nat. Nanotechnol.* **5**, 350 (2010).
23. D. M. Eigler, E. K. Schweizer. *Nature* **344**, 524 (1990).
24. S. W. Hla, K.-F. Braun, K.-H. Rieder. *Phys. Rev. B* **67**, 201402 (2003).